Random cellular structures generated from a 2D Ising ferromagnet

1992 J. Phys. A: Math. Gen. 25 6193

(http://iopscience.iop.org/0305-4470/25/23/017)

J. Phys. A: Math. Gen. 25 (1992) 6193-6210. Printed in the UK

Random cellular structures generated from a 2D Ising ferromagnet

R Delannay†, G Le Caër‡ and M Khatun§

† Laboratoire d'Energétique et de Mécanique Théorique et Appliquée, associé au CNRS, URA 875, Ecole des Mines, F 54042 Nancy Cedex, France

‡ Laboratoire de Science et Génie des Matériaux Métalliques, associé au CNRS, URA 159, Ecole des Mines, F 54042 Nancy Cedex, France

§ Department of Physics and Astronomy, Ball State University, Muncie, IN 47306-0505, USA

Received 22 November 1991, in final form 22 July 1992

Abstract. Topological models of 2D cellular structures are associated with distributions of spins given by a ferromagnetic Ising model with nearest-neighbour interactions on a square lattice. Every vertex of a square lattice is topologically unstable as it belongs to more than three polygons. There are two ways, associated with the spin states, to remove this degeneracy by replacing every vertex by one side. Topological properties such as the distribution $P(n)$ of the number n of cell sides, the two-cell correlation $M_k(n) = P(k)A_{kn}$ which is the average number of k-sided neighbours of a cell with n sides (n-cell), the mean number $m(n)$ of sides of the first neighbour cells of n-cells are characterized as a function of T/T_c by direct calculations and by Monte Carlo and $Q2R$ simulations. The correlations A_{kn} of a biological tissue are compared with the A_{kn} of a ferromagnetic Ising cellular structure and with the A_{kn} expected from the maximum-entropy model.

1. Introduction

In two previous papers (Le Caër 1991a, b, referred to hereafter as I and II), a method for constructing topological models of space-filling random cellular structures has been described and has been applied to two-dimensional structures. The models yield the relative repartition of cells and do not need or provide information about angles and cell-edge lengths.

Let us consider a lattice in which every site is characterized by its valence z ($> z_s = 3$ in 2D) which is the number of edges merging in that vertex. Every vertex, which belongs to more than three cells, is structurally unstable as its properties change by small deformations. The construction method is based on rules which allow removal of this instability. The stable configuration is obtained by adding $z-3$ sides at every vertex (figure 1, Thompson 1917). Every added side is connected at least to one added side for $z > 4$ (I and II). The latter rule produces a set of $Q(z)$ possible stable configurations, called states, which have been enumerated as a function of z in II. The last ingredient of the method is a criterion for distributing the various states on the lattice sites. In the previous work (I and II), distributions of independent states were only considered for z ranging from 4 to infinity. An equivalent method of construction of the cellular structure uses the Euler diagonal triangulation of the dual lattice (Le Caër 1991b). For a square lattice SL, it consists of triangulating (T) every square by choosing one of

0305-4470/92/236193+18$07.50

the two possible diagonals. SL is thus transformed into TSL whose dual is the associated cellular structure.

The present paper will focus on interacting states on the square lattice $z=4$ (or on any lattice topologically equivalent to it). For that lattice, $Q(4)=2$ and a 'spin' $S=\pm\frac{1}{2}$ can be introduced (I, figure 1). The spin allows description of the type of stable configuration which is chosen from the two possible at every lattice site. It further allows calculation of the topological characteristics of the cellular structure associated with the square 'mother' lattice. The latter characteristics include usually the distribution $P(n)$ of the number n of edges of cells (called here n-cells) and the n-dependence of the mean number $m(n)$ of sides of the first neighbour cells of n-cells. Very recently, Peshkin *et al* (1991) have drawn attention to a two-cell correlation: $M_k(n)$ which is the average number of k-sided neighbours of an n-cell.

$M_k(n)$ and $m(n)$ are related by (Peshkin *et al* 1991):

$$nm(n)=\sum_k kM_k(n). \tag{1}$$

A semi-empirical law, the Aboav-Weaire law (Aboav 1970, 1980, Weaire 1974), expresses that $m(n)$ is linearly related to $1/n$ by

$$m(n)=6-a+(6a+\mu_2)/n \tag{2}$$

where μ_2 is the variance of the distribution of n: $\mu_2=\langle n^2\rangle-\langle n\rangle^2$, with $\langle n\rangle=6$ as a consequence of the Euler relation in 2D (Weaire and Rivier 1984) and $\langle nm(n)\rangle=\mu_2+36$ (Weaire 1974). In many natural random cellular structures, the parameter a is of the order of 1.2 (Aboav 1980). Equation (2) has been derived by Peshkin *et al* (1991) from the application of the maximum entropy principle with constraints imposed on the $P(n)$: $M_k(n)$ are predicted to be linear in n in order to reduce the number of independent constraints. The deviations from the Aboav-Weaire law (for $n=3$ and $n\geqslant 9$) have been previously discussed for the topological models mainly associated with a distribution of independent and equiprobable states (I, II).

The purpose of the present work is to investigate the consequences of interactions on the topological properties of cellular structures associated with a distribution of spins on a square lattice. The simplest models of interacting spins are given by Ising models. At $T=0$, many of these models give rise to ordered magnetic structures which yield ordered cellular structures with only six-sided cells. This is, for instance, true for structures built from alternating strips of + and − spins with boundaries parallel to one of the square side, whatever the distribution of the strip widths. As the same cellular structure is also associated with all these models at infinite temperature, we have chosen to investigate first the best known model, that is the ferromagnetic Ising model with nearest-neighbour couplings, as a function of the reduced temperature T/T_c (the associated cellular structures are called in short ferromagnetic Ising cellular structures). Ising spin glasses are also worth studying but they raise more complex simulation problems. The $P(n)$ distributions, which were derived in paper I for the ferromagnetic Ising model, are calculated. Moreover, Monte Carlo and $Q2R$ cellular automata (Vichniac 1984, Stauffer 1991) simulations are performed in order to provide information about $M_k(n)$ and $m(n)$. The results are compared to those calculated for a random distribution of states as well as to experimental and to simulated results reported for various cellular structures with similar characteristics: $\mu_2\leqslant 1$, $P(n)$ negligible for $n=3$ and $n\geqslant 9$.

2. Previous results for the square lattice

Labelling as 1 the upper right corner of the central square in figure 1 and as 2 the upper left corner etc, the number of sides n ($4 \leqslant n \leqslant 8$) is given by ($S_j = \pm\frac{1}{2}$, I):

$$n = 6 + \sum_{j=1}^{4} (-1)^{j+1} S_j. \tag{3}$$

If we consider any square of the starting lattice, its corresponding cell (n-cell) in the topological model will have two types of neighbours (figure 1):

- 4 unconditional neighbours which are associated with the four neighbouring squares which share one side with the considered square.
- $n-4$ conditional neighbours which are associated with $n-4$ squares which share one vertex with the considered square. It is the spin value which determines which squares have to be chosen among the four possible ones. The following relation has also been derived in I:

$$nm(n, 1) = 10 + 9n/2 - \frac{1}{2}\left\{\sum_{j=1}^{4} (-1)^j M_j^+\right\} + \sum_{j=1}^{4} S_j M_j^- \tag{4}$$

where the random variable $nm(n, 1)$ is the total number of sides of the first-neighbour cells of a n-cell. The average over all configurations of spins, for a fixed n, is $nm(n)$. Both $M_j^{\pm}$ are given by an algebraic sum of three spins at every corner of the outer square (figure 1) which includes the nine interior squares. The relative position of S_j and M_j is also shown in figure 1. $M_j^{\pm}$ is the sum of the corner spin plus or minus the sum of its two neighbour spins, one per side of the outer square. The last sum in equation (4) is due to conditional neighbours which are responsible for the presence of pair correlations in that term.

For independent states or for the Ising model, all sites are equivalent. The resulting distribution $P(n)$ cannot therefore depend on the arbitrariness of the choice of the spin labelling in equation (3) and must be invariant when all spins S_j are changed to $-S_j$. All odd-moments $\mu_{2k+1} = \langle (n-6)^{2k+1} \rangle$ are zero and $P(n)$ is symmetric with respect to $n = 6$. This result is not general as spin repartitions, which give rise to asymmetrical

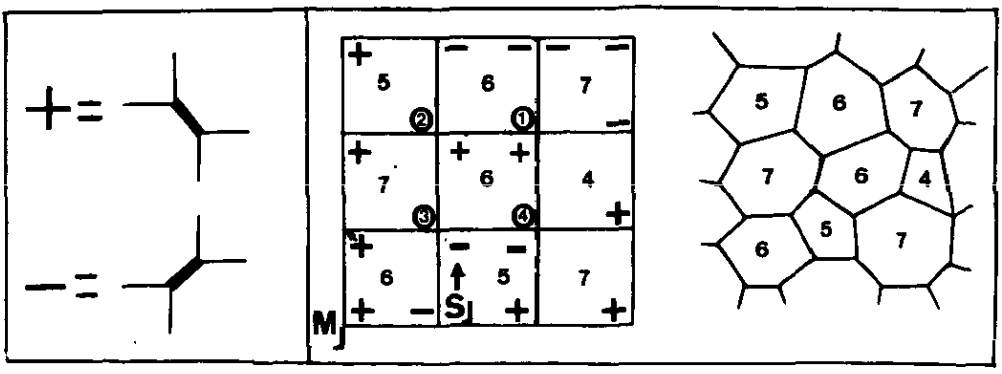

Figure 1. Left part: the two possible stable configurations (states) obtained by adding a side at a vertex of a square lattice ($+ = \frac{1}{2}$, $- = -\frac{1}{2}$). Right part: an example of a distribution of states on a square lattice, the corresponding values of the number n of cell sides and one realization of the associated cellular structure (circled numbers: labelling for equations (3) to (5)).

$P(n)$ distributions, can be easily constructed on a square lattice. Using equation (3) and averaging over all possible configurations of spins allow calculation of μ_2 and μ_4. As the even moments only depend on four spins located on the vertices of a square, they can be expressed as a function of the two pair-correlation coefficients and the quartet correlation coefficient which can be defined on that square:

$$x_1 = 4\langle S_1 S_2\rangle \qquad x_2 = 4\langle S_1 S_3\rangle \qquad x_{12} = 16\langle S_1 S_2 S_3 S_4\rangle. \tag{5}$$

As there are only two independent parameters, the pair correlation terms appear only through the combination:

$$d_{12} = 2x_1 - x_2. \tag{6}$$

We calculate (I)

$$\mu_2 = 1 - d_{12} \qquad \mu_4 = \tfrac{5}{2} + 3x_{12}/2 - 4d_{12} \tag{7}$$

and we deduce

$$\begin{aligned} P(4) &= P(8) = (\mu_4 - \mu_2)/24 = (1 + x_{12})/16 - d_{12}/8 \\ P(5) &= P(7) = (4\mu_2 - \mu_4)/6 = (1 - x_{12})/4 \\ P(6) &= 1 - (5\mu_2 - \mu_4)/4 = 3(1 + x_{12})/8 + d_{12}/4. \end{aligned} \tag{8}$$

When the spins are independently distributed on every site with a probability p for $S = \frac{1}{2}$, the correlation coefficients are given by:

$$x_1 = x_2 = d_{12} = (2\langle S_k\rangle)^2 = (2p-1)^2 = M^2 \tag{9}$$

$$x_{12} = (2\langle S_k\rangle)^4 = M^4 \qquad \mu_2 = 4p(1-p) \tag{10}$$

where M is the magnetization. For a distribution of independent states, the average of $nm(n, 1)$, for a fixed n, yields (Le Caër 1991a):

$$m(n) = p + 4 + (13 - 6p)/n + (1 - 2p)A_C(n)/n \tag{11}$$

where $A_C(n)$ is given by:

$$\begin{aligned} &A_C(4) = -1 \qquad A_C(8) = 1 \\ &A_C(5) = -(1-p)^2/(1-\mu_2/2) \qquad A_C(7) = p^2/(1-\mu_2/2) \\ &A_C(6) = (p^4 - (1-p)^4)/P(6). \end{aligned} \tag{12}$$

The Aboav-Weaire law is only exact (equations (2) and (11)) for $p = \frac{1}{2}$ with $a = 1.5$. The best least-square fits of the theoretical $nm(n)$ to the $nm(n)$ values calculated from equation (2) gives $a[nm(n)] = 1.5$ for all p (D Fraser, personal communication), while a weighted fit of $nm(n)$ with weights $P(n)$ also gives $a_W = 1.5$ (appendix A.3, equations (A.5) and (A.6)). However, if $m(n)$ deviates from the Aboav-Weaire relation, significantly different values of 'a' may be obtained from different fits to the data (II).

For the ferromagnetic Ising model, the quartet correlation function is equal to a Pfaffian of the pair correlation functions (Groeneveld *et al* 1978): $x_{12} = 2x_1^2 - x_2^2$. The pair correlations x_1 and x_2 have been determined exactly at all temperatures T/T_c (see for example Khatun *et al* 1990 and references therein). The $P(n)$ distribution can therefore be calculated from equation (8) as a function of T/T_c. The numerical results will be described in section 4 and have been used to check the validity of the computer simulations.

3. Numerical simulation methods

Equilibrium configurations $\{S_k\} = \pm\frac{1}{2}$ have been generated on a $N \times N$ square lattice, with helical boundary conditions, as a function of T/T_c using Monte Carlo simulations. The spin updating is performed sequentially according to the Glauber dynamics, going through the lattice in a regular fashion (Stauffer *et al* 1988). A probability $1/(1+\exp(\Delta E/kT))$ is used for flipping a spin S_k, where ΔE is the energy change associated with the flip of S_k into $-S_k$. The numerical simulations are performed on a HP9000/340 workstation for $N = 700$ and $0.6 \leqslant T/T_c \leqslant 0.92$ and $1.05 \leqslant T/T_c \leqslant 10\,000$. The vicinity of the Curie point has not been investigated as critical slowing down requires too long simulation times to reach equilibrium. For $T/T_c = 1.05$, configurations close to equilibrium but not truly at equilibrium have been obtained. In general, averages (tables 1 and 2) have been performed on 200 configurations once equilibrium is reached.

At high temperatures ($T/T_c \geqslant 1.179$), we have moreover used a microcanonical Ising model simulation with a $Q2R$ cellular automaton: a spin is flipped if and only if it has as many up as down neighbours (Vichniac 1984, Herrmann 1986, Stauffer 1991). For a given T/T_c, the average energy per spin $\langle E \rangle$ is proportional to the pair correlation x_1. This average energy is simply calculated for an initial random distribution of spins on the lattice with a fraction $p(s+)$ of up spins ($\langle E \rangle \alpha p(s+)(1-p(s+))$,

Table 1. Comparison between a theoretical (equations (8) and Ising correlation functions) $P(n)$ distribution at $T/T_c = 2.8616$, two distributions simulated for $p(s+) = 0.700$ ($Q2R$, 200 configurations of 65 536 cells), $T/T_c = 2.8616$ (Ising, 200 configurations of 490 000 cells) respectively and one calculated for a random distribution of spins (equations (8) to (10), $p = 0.75$) which gives the best least-squares fit to the theoretical $P(n)$.

n	$P(n)$ theoretical $T/T_c = 0.2816$	$P(n)$ ($\pm 10^{-4}$) $Q2R$ $p(s+) = 0.70$	$P(n)$ ($\pm 10^{-4}$) Ising $T/T_c = 2.8616$	$P(n)$ random $p = 0.75$
4	0.031 62	0.0316	0.0316	0.035 16
5	0.237 75	0.2378	0.2379	0.234 37
6	0.461 26	0.4613	0.4609	0.460 94
7	0.237 75	0.2377	0.2377	0.234 37
8	0.031 62	0.0316	0.0318	0.035 16

Table 2. Comparison between $m(n)$ correlations simulated for $p(s+) = 0.700$ ($Q2R$), for $T/T_c = 2.8616$ (Ising) and calculated for a random distribution of spins with $p = 0.75$ (see legend of table 1). The best least-squares fit to equation (2) yields: $a[nm(n)] = 1.348$, 1.349 and 1.5 for the $Q2R$, ferromagnetic Ising and random cases respectively. If equation (2) is valid, $m(6) = 6 + \mu_2/6 = 6.124\,06$ is expected whatever 'a'.

n	$m(n)$ $Q2R$ ($\pm 10^{-3}$)	$m(n)$ Ising ($\pm 10^{-3}$)	$m(n)$ random $p = 0.75$
4	6.868	6.869	7
5	6.416	6.417	6.46
6	6.119	6.119	6.110 17
7	5.912	5.912	5.9
8	5.760	5.760	5.75

see for example Glotzer *et al* 1990). Equating both expressions yields

$$p(s+) = 0.5 \pm 0.5(x_1)^{1/2}. \tag{13}$$

Using equation (13) (for instance with the + sign), we deduce the total number of up spins $p(s+)N^2$ which are initially randomly distributed on the sites of the $N \times N$ square ($p(s+) = 0.85$ for $T/T_c = 1.179$). The spin updating is performed with a multi-spin-coding program (Herrmann 1986) on a Macintosh SE/30 microcomputer for $N = 256$. In all cases, uniform random numbers are provided by a new portable pseudo-random number generator, with a period of $\sim 2^{144}$ (Marsaglia *et al* 1990).

4. Simulation results

Whatever T/T_c, the simulated $P(n)$ distributions are in very good agreement with the theoretical $P(n)$ calculated from equations (8) and from the numerical values of x_1, x_2 and x_{12} (figure 2(*a*)) as shown, for instance, by table 1 for $T/T_c = 2.8616$. We have observed that the theoretical $P(n)$ distributions can be accurately approximated by equations (8) to (10), that is by $P(n)$ distributions which result from a distribution of independent spins on the lattice, with a probability p shown on figure 2(*b*) as a function of T_c/T. As discussed by Khatun *et al* (1990), there is a vertical inflection point as a weak singularity of energy type $\varepsilon \log \varepsilon$ where $\varepsilon = |T - T_c|/T_c$ for all correlations, in particular for x_1, x_2, x_{12}, at the critical temperature. This type of singularity therefore exists for $P(n)$ (equations (8)).

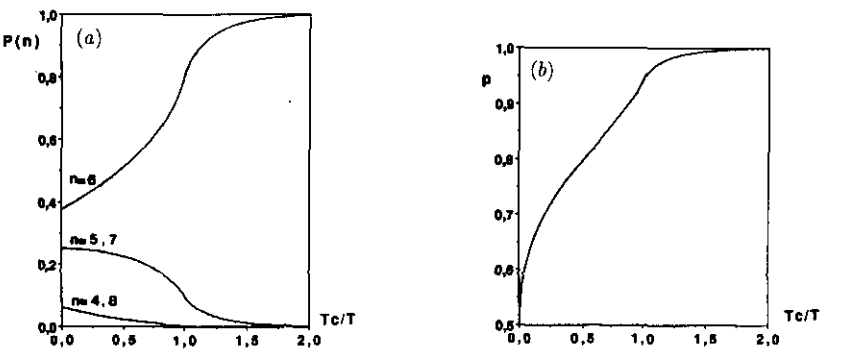

Figure 2. (*a*) *$P(n)$ distributions as a function of T_c/T for a ferromagnetic Ising model on a square lattice for $n = 4$, 8 (lower curve), $n = 5$, 7 (intermediate curve) and $n = 6$ (upper curve);* (*b*) probability $p(T_c/T)$ which gives the best least-squares fit of the theoretical $P(n)$ to $P(n)$ calculated with the help of equations (8) to (10).

Figure 3 shows the two-cell correlations $M_k(n)$, average numbers of k-sided neighbours of an n-cell, at various temperatures. The $M_k(n)$ do not all vary linearly with n even at infinite temperature at which the Aboav–Weaire law is exact with $a = 1.5$ (Le Caër 1991a). Comparisons with $M_k(n)$ correlations observed in natural and in simulated tissues are presented in section 5. At $T = \infty$, the $M_k(n)$ are (appendix A.1 and A.3)

$$M_k(n) = P(k)[n + k - 6 - 1.5(n-6)(k-6) + \tfrac{4}{9}(n-5)(n-7)(k-5)(k-7)]. \tag{14}$$

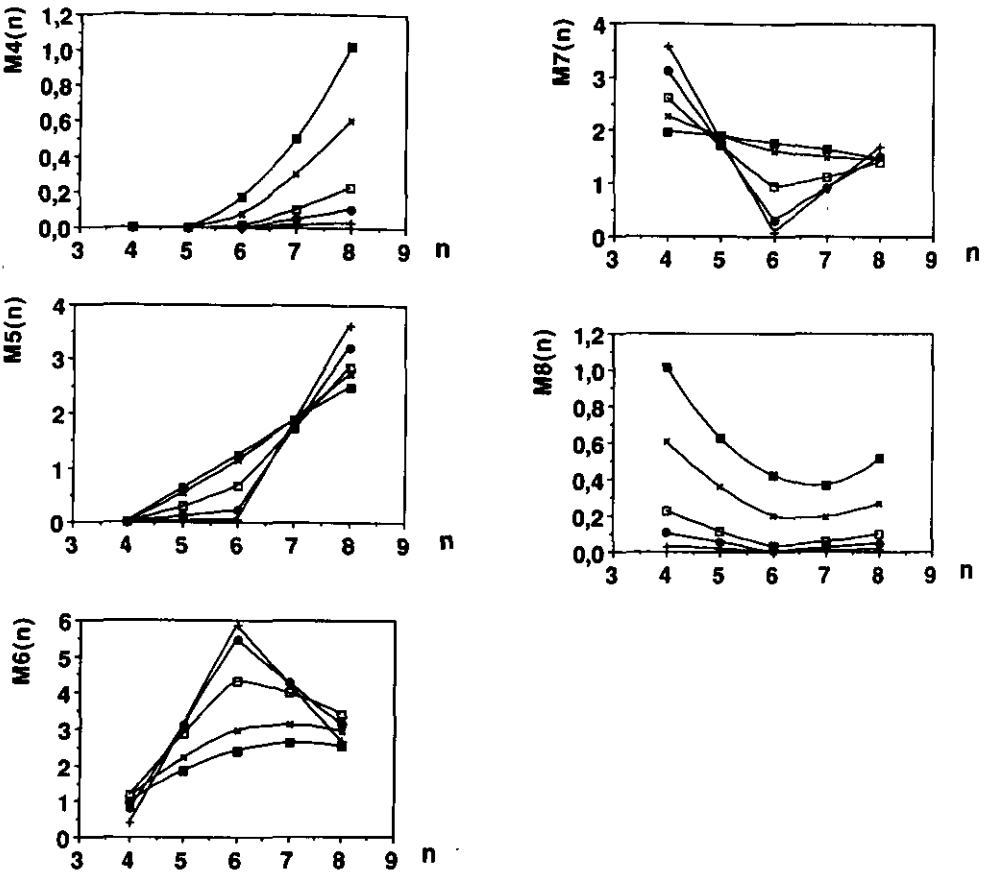

Figure 3. Correlations $M_k(n)$ for ferromagnetic Ising cellular structures at various reduced temperatures $t = T/T_c$ (full circles $t = 0.918$, open squares $t = 1.16$, crosses $t = 0.712$, crosses at 45° $t = 2.862$, full squares $t = \infty$; interpolating bold lines have been drawn for the sake of clarity).

The distribution $P(n)$ for $p = 0.5$ is very close to the maximum entropy distribution subject to the same constraints (appendix A.1 and A.5). The general expressions which allow calculating $M_k(n)$ for a distribution of independent states on a square lattice are given in appendix A.1.

The correlations $m(n)$ provided by the Monte Carlo and the $Q2R$ simulations are in good agreement at high temperatures, as shown for instance by table 2 for $T/T_c = 2.8616$ which also gives the $m(n)$ values calculated for a random distribution of spins with $p = 0.75$ (equations (11) and (12)). Two cellular structures associated respectively with an independent distribution of spins and with a ferromagnetic Ising model, which show almost identical side distributions $P(n)$, differ in the intercell correlations and in $a[nm(n)]$ (figure 4). The differences between the latter correlations, which are generally rather small, pass through an extremum around or at T_c for $n = 4, 5, 7, 8$. The correlations $m(6)$ are very close for the two structures (figure 4). Figure 4 suggests the existence of weak singularities for $m(6)$ and $m(7)$ at the critical point while extrema are observed for the other $m(n)$. The correlations $M_k(n)$ show much larger relative variations than $m(n)$ (figures 3 and 4), both being related by equation (1).

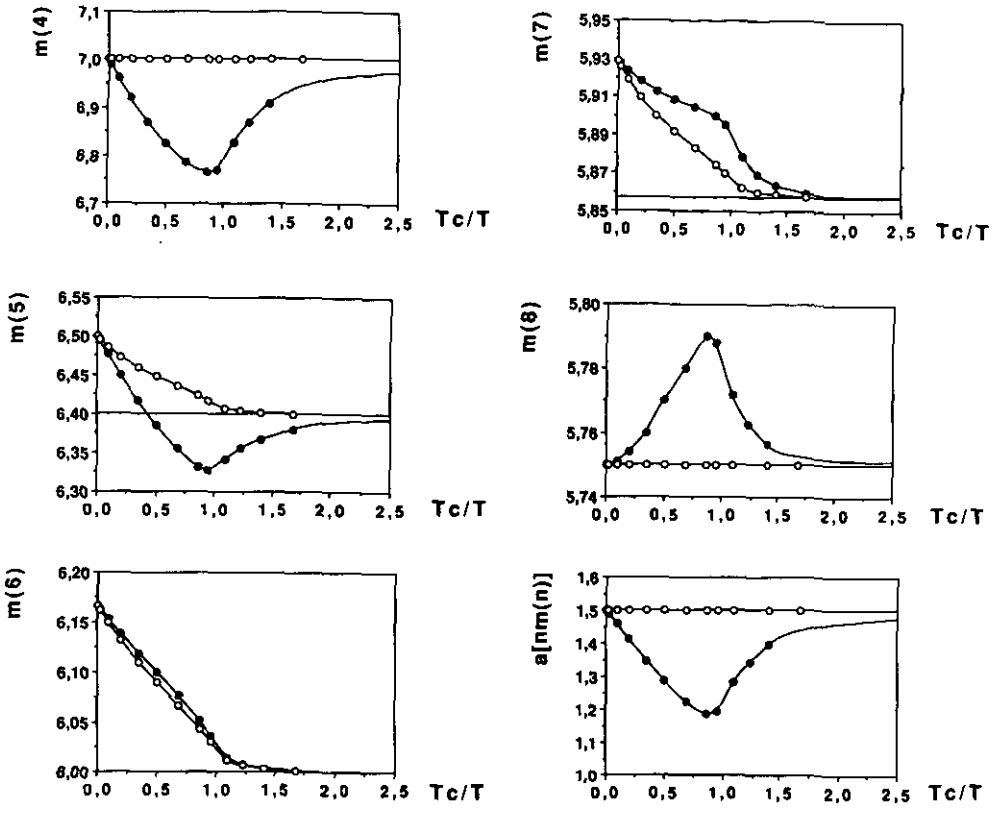

Figure 4. Correlations $m(n)$ and best least-squares value of $a[nm(n)]$ (equation (2)) as a function of T_c/T (horizontal lines: $m(n)$ values calculated from equations (11) and (12) for $p=0$ or 1, full circles: ferromagnetic Ising model, open circles: random distribution of a fraction $p(T_c/T)$ of up spins as given in figure 2(*b*); bold lines are guides for the eyes). The errors are less than the point sizes.

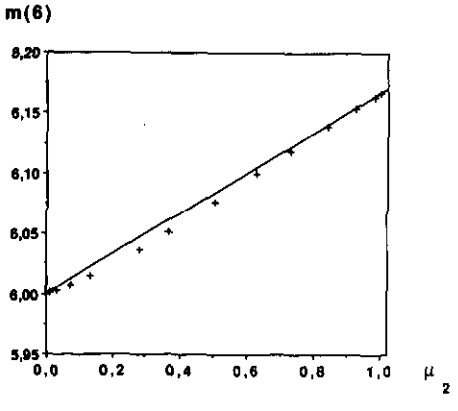

Figure 5. $m(6)$ versus μ_2 (crosses: simulation results for the ferromagnetic Ising structure, bold line: $m(6)=6+\mu_2/6$).

When the temperature goes to zero, the intercell correlations are expected to become identical for the two latter types of cellular structures ($p \to 0$ or $p \to 1$). The $m(n)$ values calculated from equations (11) and (12) for $p = 0$ or 1 ($m(4) = 7$, $m(5) = 6.4$, $m(6) = 6$, $m(7) = \frac{41}{7} \approx 5.8571$, $m(8) = 5.75$) are in fact observed to be the best extrapolated values of the Ising $m(n)$ versus μ_2 plots when μ_2 goes to zero. The Aboav-Weaire law predicts that $m(6) = 6 + \mu_2/6$ whatever a. Figure 5 shows that $m(6)$ is well approximated by the latter relation with a maximum deviation of $\approx 0.15\%$. The best least-squares fit of $nm(n)$ to $nm(n)$ given by equation (2) allows us to calculate $a[nm(n)]$ (close to a_W (A.5), figure 4) which decreases from 1.5 to ≈ 1.2 at the critical point. The temperature dependences of $m(4)$ and of $a[nm(n)]$ are strikingly similar. In fact, a plot of 'a' as a function of $m(4)$ seems to indicate that these two parameters are in a one to one correspondence.

5. Comparison with natural and other simulated cellular structures

Various natural or simulated cellular structures exhibit distributions of the number of cell sides $P(n)$ mainly with $4 \leqslant n \leqslant 8$ and $\mu_2 \leqslant 1$. This is the case for various undifferentiated biological tissues (Lewis 1931, Mombach *et al* 1990), for cellular arrays obtained in directional solidification of alloys (Billia *et al* 1991, Jamgotchian *et al* 1991) or for Voronoi tessellations calculated during the course of constant pressure Monte Carlo simulations of 2D hard disks at various packing fractions η (Fraser *et al* 1990). The $P(n)$ distributions observed in such natural or simulated cellular structures agree satisfactorily with the distributions calculated from the topological models associated with a distribution of independent states on a square lattice (Le Caër 1991a). The need to confirm that the correlations between cells are correctly represented by the topological models was however emphasized. The present results corroborate these statements as shown by tables 3 and 4 for $P(n)$ distributions with different values of μ_2. The distributions (table 3) calculated with various models, but all with $\mu_2 = 0.812$, show only minor differences while they agree reasonably with the experimental distribution for the cucumber (figure 6). As expected, the calculated distributions agree more and more closely when μ_2 decreases: when $P(4)$ and $P(8)$ are vanishingly small, μ_2

Table 3. *Comparison between experimental and calculated distributions of the number of cell sides $P(n)$ with $\mu_2 = 0.812$:*

- *$P(n)$ for the epidermal epithelium of a 220 mm cucumber (1000 cells, Lewis 1931);*
- *$P(n)$ for the ferromagnetic Ising model on a square lattice and $T/T_c = 4.289\,82$;*
- *$P(n)$ for a random distribution of states on a square lattice and $p = 0.716\,795$;*
- *$P(n)$ deduced from the application of the maximum entropy principle with the sole constraints $\langle n \rangle = 6$ and $\mu_2 = 0.812$ ($P(3) \approx 1.74 \times 10^{-3}$, $P(10) = 2.34 \times 10^{-5}$).*

n	220 mm cucumber	Ising	Random	Maximum entropy
4	0.025 ± 0.010	0.040 34	0.041 21	0.037 75
5	0.279 ± 0.028	0.244 62	0.241 16	0.239 21
6	0.415 ± 0.031	0.430 07	0.435 25	0.442 63
7	0.237 ± 0.027	0.244 62	0.241 16	0.239 16
8	0.040 ± 0.012	0.040 34	0.041 21	0.037 73
9	0.004 ± 0.004	0	0	1.738×10^{-3}

Table 4. Comparison between experimental and calculated distributions of the number of cell sides $P(n)$ with $\mu_2 = 1$:

- $P(n)$ for a cellular tissue in a human amnion (1000 cells, Lewis 1931);
- $P(n)$ deduced from the application of the maximum entropy principle with the constraints $\langle n \rangle = 6$ and $\mu_2 = 1$;
- $P(n)$ for a random distribution of states on a square lattice and $p = 0.5$ (Ising for $T/T_c = \infty$).

n	3	4	5	6	7	8	9
Human amnion	0.004 ± 0.004	0.054 ± 0.014	0.248 ± 0.027	0.397 ± 0.031	0.241 ± 0.027	0.049 ± 0.014	0.007 ± 0.005
Maximum entropy	0.004	0.054	0.242	0.399	0.242	0.054	0.005
Random $p = 0.5$	0	6.25×10^{-2}	0.25	0.375	0.25	6.25×10^{-2}	0

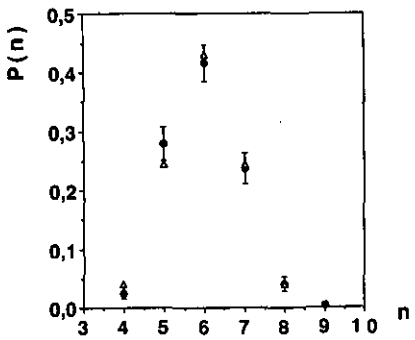

Figure 6. Distribution $P(n)$ of the number n of edges of cells for an epidermal epithelium of a 220-mm cucumber (full circles with error bars, Lewis 1931) and for the ferromagnetic Ising model on a square lattice at $T/T_c = 4.289\,82$ (open triangles, table 3).

determines $P(5)$ and $P(7)$ almost uniquely. Table 4 emphasizes the striking similarities between the $P(n)$ distribution for a cellular tissue in a human amnion (Lewis 1931) and the maximum entropy distribution (Rivier 1985) calculated with the sole constraints $\langle n \rangle = 6$ and $\mu_2 = 1$ (II). We conclude that a detailed comparison between the correlations among cells is absolutely necessary before assessing the relevance of a model. As the data which are needed in order to perform such comparisons are only available for the epidermal epithelium of a 220-mm cucumber (Lewis 1931) and for the 2D hard-disk simulations (Fraser 1990, personal communication), the following discussion will be mainly restricted to these two cellular structures.

Mombach *et al* (1990) have determined $P(n)$ and $m(n)$ as a function of n in various vegetable tissues. The distributions $P(n)$ calculated from a ferromagnetic Ising model cannot account for the experimental disymmetries in $P(5)$ and $P(8)$ (see also table 3) but give an overall acceptable description of such $P(n)$. The experimental $m(8)$ are slightly but systematically lower than the $m(8)$ expected from the Aboav-Weaire law with $a = 1$ (figure 4 of Mombach *et al* 1990). Deviations also exist for $m(7)$ in the cases of onion and of aloe and for $m(4)$ in the case of Anthurium. A better knowledge of experimental uncertainties would be necessary before concluding to the strict validity of the Aboav-Weaire law.

In order to compare in detail the two cellular structures '220-mm cucumber' and 'ferromagnetic Ising', we have simply determined the only free parameter of the model, that is the temperature T/T_c, from the experimental value of μ_2 for the cucumber tissue, $\mu_2 = 0.812$ (Lewis 1931, table 3, $T/T_c = 4.289\,82$). For the '2D hard disk' tissue, we have used the results of a simulation performed for the packing fraction $\eta = 0.492$ which yields $P(n)$ ($P(4) = 0.014$, $P(5) = 0.250$, $P(6) = 0.49$, $P(7) = 0.216$, $P(8) = 0.028$, $P(9) = 0.002$, 81 600 cells, Fraser 1990, personal communication), in reasonable agreement with the experimental ones (table 3). We have calculated the correlations $M_k(n)$ ($4 \leqslant k \leqslant 8$) for the three previous cellular structures. Besides equation (1), the $M_k(n)$ must also obey the following relations (Peshkin *et al* 1991):

$$\sum_k M_k(n) = n \tag{15}$$

$$P(k)M_n(k) = P(n)M_k(n). \tag{16}$$

Summing up equation (15) over n and using (14) yields

$$\sum_n P(n)M_k(n) = P(k)\sum_n M_n(k) = kP(k). \tag{17}$$

The topological correlation functions A_{kn} defined as

$$A_{kn} = M_k(n)/P(k) = M_n(k)/P(n) = A_{nk} \tag{18}$$

allow comparing topological properties of tissues which show different distributions $P(n)$ of the number of edges of cells. The symmetry is a consequence of relation (16) while relations (15) and (1) become

$$\langle A_{kn}\rangle = \sum P(k)A_{kn} = n \qquad \langle kA_{kn}\rangle = nm(n). \tag{19}$$

If P_{kn} is the probability that a cell with k sides and a cell with n sides are neighbours, the correlation A_{kn} is

$$A_{kn} = 6P_{kn}/(P(k)P(n)). \tag{20}$$

Fradkov *et al* (1987) have defined the topological gas as an ideal arrangement of cells free of correlations with

$$P_{kn} = knP(k)P(n)/36 \qquad A_{kn} = kn/6 \tag{21}$$

that is (Fradkov *et al* 1987, relation (19)):

$$m(n) = 6 + \mu_2/6 \tag{22}$$

and $a = -\mu_2/6$ (equation (2)). If the A_{kn} are linear in k and in n, they are uniquely expressed as (appendix A.2)

$$A_{kn} = n + k - 6 - (a/\mu_2)(n-6)(k-6) \tag{23}$$

where a is the parameter of the Aboav–Weaire law (equation (2)).

Relation (23) does not imply that the associated distribution $P(n)$ maximizes the entropy, $S = -\Sigma\, P(n)\log(P(n))$, subject to the two remaining independent constraints: $\langle 1\rangle = \Sigma\, P(n) = 1$ and $\langle n\rangle = 6$, as the maximum entropy is only reached for the distribution $P_m(n) = 0.75^{(n-3)}/4$ ($n \geqslant 3$) which has very unusual features such as a mode at $n = 3$ and a large $\mu_2 = 12$. Besides the constraints defined by equations (19) (see also appendix A.4), the topological correlation functions A_{kn} must fulfil the unavoidable condition

$$A_{kn} \geqslant 0. \tag{24}$$

Extra constraints exist for tessellations with convex polygons such as Voronoi or Laguerre (Telley 1989) tessellations:

$$A_{33} = 0 \tag{25}$$

as two triangular cells cannot share a side without creating at least one neighbouring concave cell. By construction, the topological models described in II also have

$$A_{33} = 0 \qquad A_{34} = 0 \text{ (if all } z_i \geq 4). \tag{26}$$

The latter constraints may be too stringent for some natural structures but constitute in many cases reasonable approximations (e.g. polycrystal cuts) as the energetic cost of $A_{33} \neq 0$ may be locally too high.

Using a maximum-entropy argument, Peshkin *et al* (1991) have predicted that $M_k(n)$ is linear in n (only the two constraints $\langle 1 \rangle = 1$ and $\langle n \rangle = 6$ are independent):

$$M_k(n) = C_k + D_k n. \tag{27}$$

Using equations (18) and (23), we derive

$$C_k = P(k)(k-6)\{1 + 6a/\mu_2\} \tag{28}$$

$$D_k = P(k)\{1 - (k-6)a/\mu_2\}. \tag{29}$$

However equations (27) to (29) do not guarantee that $M_k(n) \geq 0$ for all allowed values of k and n ($n_1 \leq n$, $k \leq n_2$). For instance, if $P(3) \neq 0$, $M_3(3) = -9P(3)a/\mu_2$ will be positive only for $a < 0$ while a is positive and of the order of 1 in most natural cellular structures. For $a > 0$ and $n_1 = 3$, $M_3(n)$ cannot be linear in the whole range $[n_1, n_2]$ and must show an upwards curvature for small values of n. If we consider n (or k) as a continuous variable (not restricted to be >0), we observe that the point n (or $k) = 6 + \mu_2/a$, $A_{kn} = 6 + \mu_2/a$ belongs to all the lines $A_{kn} = g_k(n)$ (or $= g_n(k)$). If $n_1 = 3$ and if n_2 is infinite, it is therefore only for $-\frac{1}{3} \leq a/\mu_2 \leq 0$ that $M_k(n)$ will satisfy the positivity constraint (relation (24)) whatever k and n. For $a > 0$ and k large, $M_k(n)$ may also become negative for $n > 6$ and again $M_k(n)$ will curve in order to fulfil the positivity constraint. Such distortions are also expected to propagate to other $M_k(n)$ correlations and may produce departures from the Aboav–Weaire law particularly for $n = 3$.

Exact calculations of the correlation functions A_{kn} have been performed in various topological models for $n_1 = 3$ and n_2 up to 46 (DIES). A surprising overall quantitative agreement is observed to hold between the A_{kn} for $z = 5$ and the experimental A_{kn} of cuts of alumina polycrystals (Le Caër and Delannay 1992). Moreover, the correlation functions for $n_2 \geq 14$ (for instance, topological models associated with 8-8-4, 3-12-12 Laves tilings, II, Grünbaum and Shephard 1987) clearly show the curvatures and distortions aforementioned. Peshkin *et al* (1991) also report that a substantial curvature becomes visible at small n, especially for large k, in a case with $a = 0.49$. The simulation results of figure 2 of Peshkin *et al* (1991), which corresponds to $k \leq 18$ and $a = -0.03$, as well as their simulations with $a < 0$ ($a = -1.33$, -0.96) do not suffer much from the previous difficulties and have $M_k(n) \geq 0$ with only negligible departures from linearity. However, the corresponding $P(n)$ distribution has an unusually large μ_2 ($=12.69$) for $a = -1.33$ which is in fact not so different from $\mu_2 = 12$ which is calculated for the maximum entropy distribution $P_m(n)$.

As $P(k)$, $a[nm(n)]$ ($=1.23$) and μ_2 ($=0.812$) are known for the cucumber tissue, equation (23) can be used to calculate A_{kn} (figure 7). Care has been (and must generally be) taken in the determination of experimental A_{kn} for small values of $P(k)$ in order

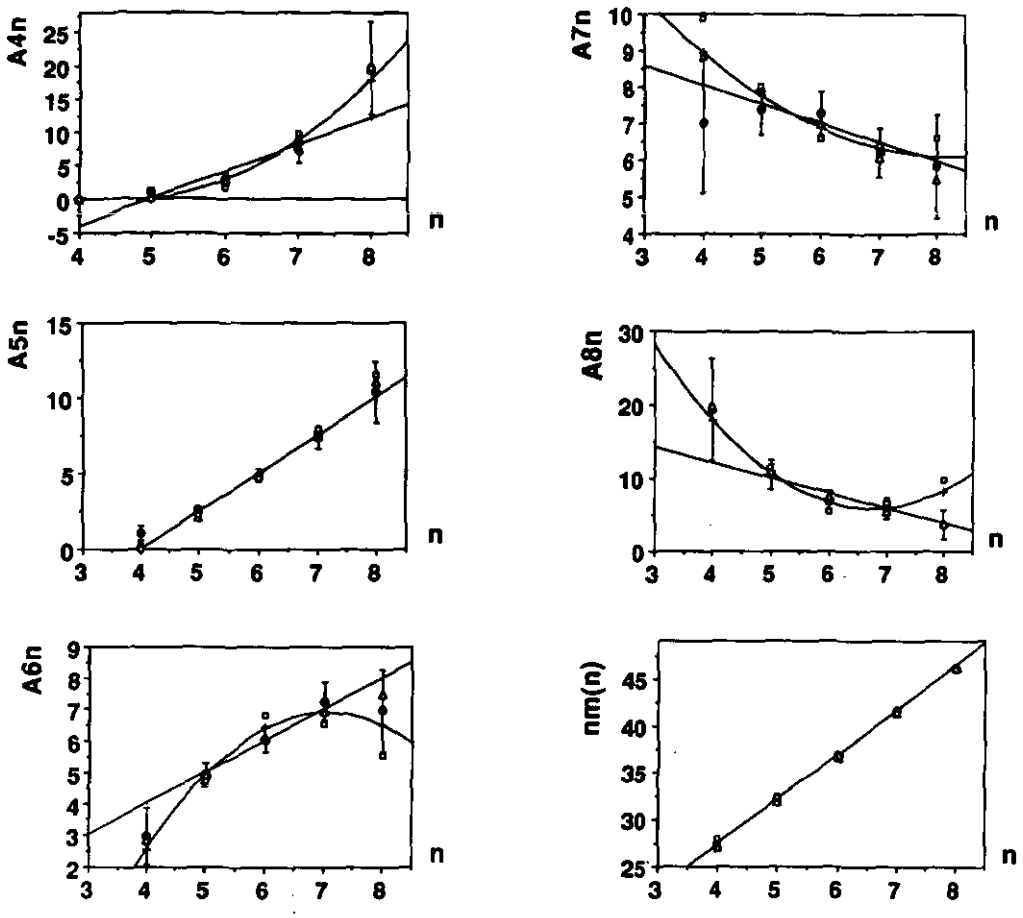

Figure 7. Correlations A_{kn} and $nm(n)$ (all A_{kn} have been represented for the sake of clarity, in spite of the symmetry $A_{kn} = A_{nk}$): (*a*) for an epidermal epithelium of a 220-mm cucumber (full circles with error bars, calculated from data of Lewis 1931); (*b*) for a ferromagnetic Ising cellular structure at $T/T_c = 4.2898$ (crosses and associated bold line, errors less than the cross size); (*c*) for a cellular structure associated with a distribution of independent states on a square lattice (open squares, $p = 0.716\,795$, $\mu_2 = 0.812$, exact values from relations (A.2)); (*d*) for the Voronoi tessellation calculated from a simulation of a hard-disk fluid at a packing fraction $\eta = 0.492$ (open triangles, errors about 10 times less than the corresponding errors for the A_{kn} of the cucumber, Fraser 1990, personal communication); (*e*) linear correlations (maximum entropy) calculated from equation (23) with $a = 1.23$ and $\mu_2 = 0.812$ (straight lines).

to avoid calculating non-significant values which would be obtained by dividing $M_k(n)$ by a $P(k)$ determined from a too small number of cells. An overall trend towards a decrease of A_{kn} with n is observed for $k \geqslant 7$ for all structures on figure 7, as also expected from equation (23). For the epidermal epithelium of the cucumber, the experimental A_{kn} have been derived from the numerical values given in table 4 of Lewis (1931). There is a striking qualitative agreement, and even quantitative agreement for almost all n values, between the two-cell correlations determined for the three structures and for the maximum entropy model. Although the ferromagnetic Ising structure is an oversimplified model of such natural structures, as it constrains the $P(n)$ distributions to be symmetric and as it forbids cells with three sides or with nine

sides or more, it seems to share some general topological characteristics with the previous tissues.

We are clearly unable to decide if the experimental A_{kn} are curved as are the correlation functions of the Ising and hard-disk structures or if they are essentially linear as predicted by the maximum entropy model. In any case, the latter model cannot be exact for A_{4n} as it predicts negative values of A_{44} when $a/\mu_2 \geq 0.5$ (here $a/\mu_2 \sim 1.51$, A_{44} (maximum entropy) ~ -4, figure 7) and distortions must take place. Moreover, the linearity of A_{kn} in k and in n does not imply that the entropy is maximum if $P(n)$ differs from $P_m(n)$ calculated in the way discussed after equation (23) with eventual extra conditions about the allowed range of n: $n_1 \leq n \leq n_2$, or including prior probabilities.

More important is the fact that the A_{kn} seem to be the relevant correlation functions to be considered as the $M_k(n)$ show larger relative differences than the A_{kn} which are mainly due to differences in the $P(k)$ factors. Structures with not too different $P(n)$, $n_1 \leq n \leq n_2$, a and μ_2 topological characteristics share similar correlations A_{kn} although they belong to very different fields. The latter conclusion is confirmed for larger values of μ_2 and for $n_1 = 3$, $n_2 \geq 12$ (up to 46, Le Caër and Delannay 1992). This may be consistent with a trend towards the constrained maximization of entropy with, in general, deviations of A_{kn} from the linear behaviour. The correlation functions exhibit a regular behaviour (figure 7): A_{4n} is curved upwards at least for the Ising and hard-disk structures. The overall curvature decreases when k increases and A_{5n} is almost linear in n while A_{6n} is curved downwards. As will be shown in a forthcoming publication for $n_1 = 3$ and $n_2 \geq 12$ (Delannay and Le Caër 1992), the surface obtained when plotting A_{kn} as a function of k and n is very smooth and changes progressively when k (or n) increases.

Further theoretical work which takes into account the positivity constraint in the frame of the maximum entropy method is necessary in order to take full profit of the heuristic power of the latter method. This would help us to know if the evolution of some structures towards a maximum entropy state is hindered or if some constraints have not yet been identified. Finally, more precise experiments are needed for biological tissues and more generally for structures with $\mu_2 \leq 1$.

6. Conclusions

The topological properties of cellular structures associated with a ferromagnetic Ising model on a square lattice have been characterized as a function of temperature. The relative variations of $m(n)$ are on the whole rather small ($\leq 3.6\%$) while the $a[nm(n)]$ parameter of the Aboav–Weaire law decreases by $\sim 20\%$ and reaches its minimum at the critical temperature which would be worth investigating in detail using cluster algorithms. The correlations $M_k(n)$ are more sensitive to temperature variations but the A_{kn} differ little from the A_{kn} calculated for random distributions of spins (relations (A.2) with $p(T_c/T)$ given by figure 2(b)). We observe that qualitative and overall fair quantitative agreements hold between the A_{kn} of the ferromagnetic Ising model, the A_{kn} of an epidermal epithelium of a cucumber (Lewis 1931) and the A_{kn} of a Voronoi tessellation generated from a 2D hard-disk fluid for a packing fraction $\eta = 0.492$ (Fraser *et al* 1990). More precise experimental characterizations of topological properties of natural 2D cellular structures, including in particular A_{kn} for small and large values of n, are desirable in order to ascertain the validity of theoretical models. Unfortunately, no theory is presently able to predict both $P(n)$ and A_{kn} beforehand.

Acknowledgments

We wish to thank Dr D P Fraser (McGill University, Montréal, Canada, now at NERC Computer Services, Plymouth, UK) for the communication of detailed numerical results of her 2D hard-disk simulations, Professor A Mocellin (Ecole des Mines de Nancy) for useful discussions and Dr N Rivier (Imperial College, London) for useful comments.

Appendix A

We define A_{kn} as (equation (18))

$$A_{kn} = M_k(n)/P(k) = A_{nk} \tag{A.1}$$

A.1. For a distribution of independent states on a square lattice with a fraction p (or $1-p$) of up spins, the A_{kn} are calculated exactly as a function of $\mu_2 = 4p(1-p)$:

defining $G_5 = 2-\mu_2$ and $G_6 = 1-\mu_2+0.375\mu_2^2$

$$A_{44} = A_{45} = 0 \qquad A_{46} = \mu_2/G_6 \qquad A_{47} = 8/\mu_2 \qquad A_{48} = 16/\mu_2$$

$$A_{55} = (12-7\mu_2)/\{2G_5^2\} \qquad A_{56} = (48-44\mu_2+11\mu_2^2)/(8G_5G_6)$$

$$A_{57} = (32-16\mu-\mu_2^2)/(2\mu_2G_5^2) \qquad A_{58} = (16-6\mu_2)/(\mu_2G_5) \tag{A.2}$$

$$A_{66} = (192-304\mu_2+168\mu_2^2-27\mu_2^3)/(32G_6^2)$$

$$A_{67} = (64-56\mu_2+13\mu_2^2)/(8G_5G_6) \qquad A_{68} = (4+\mu_2)/(2G_6)$$

$$A_{77} = (16+4\mu_2-7\mu_2^2)/(2\mu_2G_5^2) \qquad A_{78} = (8-2\mu_2)/(\mu_2G_5) \qquad A_{88} = 8/\mu_2.$$

The rank of the (7×5) matrix A deduced from the constraints on $P(k)$ (Peshkin *et al* 1991, equation 16), whose elements are: $A(1,j)=1$, $A(2,j)=j$, $A(i,j)=A_{i+1,j}$ ($i=3,\ldots,7$, $j=4,\ldots,8$) is equal to 3 whatever μ_2 ($\neq 0$). The A_{kn} given by (A.2) differ little (figure 7) from the A_{kn} of ferromagnetic Ising cellular structures, with $p(T_c/T)$ given by figure 2(*b*).

A.2. Let us assume that $M_k(n)$ is linear in n (relation (27)). Peshkin *et al* (1991) have deduced that $C_6 = 0$ and that $D_k/P(k) = F_k$ is linear in k. Relation (27) yields ($E_k = C_k/P(k)$)

$$A_{kn} = E_k + nF_k.$$

As $A_{kn} = A_{nk}$, A_{kn} is linear both in n and in k. Using particular values of n, it is readily shown that E_k and F_k are linear in k. Therefore

$$A_{kn} = \alpha kn + \beta(n+k) + \delta. \tag{A.3}$$

From the condition $\langle A_{nk}\rangle = k$, we deduce that $k = E_k + 6F_k = A_{k6}$ whatever k and consequently that $6\alpha+\beta = 1$ and $6\beta+\delta = 0$: β and δ are therefore expressed as a function of the sole parameter α. Using the second condition (19), $\langle kA_{kn}\rangle = nm(n)$, we obtain

$$nm(n) = n(6+\alpha\mu_2) + \mu_2(1-6\alpha)$$

which is the Aboav-Weaire law (equation (2)) with $\alpha = -a/\mu_2$. Finally, A_{kn} is uniquely given by the linear form (relation (23))

$$A_{kn} = n+k-6-(a/\mu_2)(n-6)(k-6).$$

A.3. More generally, *if the A_{kn} are polynomials* of degree L in k and in n, they are conveniently expressed as a function of $L(L+1)/2$ coefficients

$$A_{kn} = n + k - 6 + \sum_{i=1}^{L} \sum_{j=1}^{i} C_{ij}[k_i n_j + k_j n_i] \tag{A.4}$$

with

$$x_i = (x-6)^i - \mu_i \qquad \mu_i = \sum_k P(k)(k-6)^i \qquad \mu_0 = 1,\ \mu_1 = 0.$$

It is readily verified that the A_{kn} given by equation (A.4) satisfy the required constraints (conditions (19)):

$$A_{kn} = A_{nk}$$

as

$$\langle k_i \rangle = \sum_k P(k)[(k-6)^i - \mu_i] = 0$$

$$\langle A_{kn} \rangle = \sum_k P(k) A_{kn} = n$$

as $\langle k_i k_j \rangle = \mu_{i+j} - \mu_i \mu_j$

$$\langle k A_{kn} \rangle = nm(n) = 6n + \mu_2 + \sum_{i=1}^{L} \sum_{j=1}^{i} C_{ij}[\mu_{i+1} n_j + \mu_{j+1} n_i]$$

and as $\langle n_j \rangle = 0$, we calculate

$$\langle nm(n) \rangle = \sum_n P(n) nm(n) = \mu_2 + 36$$

as expected from the Weaire sum rule (Weaire 1974). When the Aboav–Weaire law does not hold, that is when $nm(n)$ is not linear in n, it is easy and convenient to calculate a slope $6 - a_W$ (equation (2)) from a weighted least-squares fit of $nm(n)$ with weights $W_n = P(n)$:

$$a_W = (216 + 12\mu_2 - \langle n^2 m(n) \rangle)/\mu_2. \tag{A.5}$$

If the A_{kn} are polynomials (equation (A.4)), the application of relation (A.5) yields

$$a_W/\mu_2 = -2 \sum_{i=1}^{L} \sum_{j=1}^{i} C_{ij} r_{i+1} r_{j+1} \tag{A.6}$$

with $r_i = \mu_i/\mu_2$.

For $p = 0.5$ (DIES), the A_{kn} are given by equation (A.4) with $C_{11} = -0.75$, $C_{21} = 0$ and $C_{22} = \frac{4}{9}$ (equation (14)). As $\mu_2 = 1$, the factors $(x-6)^2 - \mu_2 = (x-5)(x-7)(x = k, n)$ explain why the A_{5n} and A_{7n} correlations are linear in n. As $P(n)$ is symmetric, $\mu_3 = 0$ and only C_{11} enters in relation (A.6) to give $a_W = -2C_{11} = 1.5$. The polynomial form given by equation (A.4) may more generally provide a useful approximation for some actual correlation functions (Delannay and Le Caër 1992).

A.4. The following relations, which are consequences of $\langle A_{kn} \rangle = n$, are valid whatever A_{kn} ($\langle\langle A_{kn} \rangle\rangle = 6$):

$$\langle\langle k_j A_{kn} \rangle\rangle = \mu_{j+1} \tag{A.7}$$

where $\langle\langle \ldots \rangle\rangle$ means average over k and n (the Weaire sum rule is obtained when one averages first over k for $j=1$). Writing A_{kn} as

$$A_{kn} = n + k - 6 + F(k, n) \tag{A.8}$$

with $F(k, n) = F(n, k)$ and averaging over k or over n, we deduce

$$\langle F(k, n)\rangle = 0. \tag{A.9}$$

Averaging $k_j F(k, n)$ over k yields a function of n

$$G_j(n) = \langle k_j F(k, n)\rangle \tag{A.10}$$

which must satisfy

$$\langle G_j(n)\rangle = 0 \qquad \text{whatever } j \tag{A.11}$$

while (equation (A.5))

$$a_W = -\langle\langle knF(k, n)\rangle\rangle/\mu_2 .$$

Relations (A.9) to (A.11) are verified if an only if (Delannay and Le Caër 1992)

$$F(k, n) = \sum_{i,j} C_{ij}[f_i(k)f_j(n) + f_i(n)f_j(k)] \tag{A.12}$$

with $\langle f_m(k)\rangle = 0$ (for instance: $f_m(k) = u_m(k) - \langle u_m(k)\rangle$).

A.5. The distribution $P_{\mathrm{ME}}(i)$ $(4 \leqslant i \leqslant 8)$ which maximizes the entropy $S = -\sum P(i)\log(P(i))$ subject to the constraints given by the previous matrix $\boldsymbol{A}$ (for $\mu_2 = 1$, appendix A.1) is also symmetric and has the same $m(n)$ correlations as the DIES distribution:

$$P_{\mathrm{ME}}(4) = P_{\mathrm{ME}}(8) = 1/(8 + 2\times 6^{0.75}) \approx 0.063\,83$$

$$P_{\mathrm{ME}}(5) = P_{\mathrm{ME}}(7) = 3/(6 + 4\times 6^{0.25}) \approx 0.244\,69$$

$$P_{\mathrm{ME}}(6) = 1/(4/3 + 2/6^{0.25}) \approx 0.382\,96.$$

As the rank of $\boldsymbol{A}$ is 3 and as the A_{kn} are polynomials of degree 2, $P_{ME}(i)$ maximizes the entropy subject to the constraints

$$\sum P(i) = 1 \qquad \langle n\rangle = 6 \text{ and } \mu_2 = 1.$$

The entropy calculated for a distribution of independent and equiprobable states

$$S_{\mathrm{DIES}} \approx 1.407\,532$$

for

$$P_{\mathrm{DIES}}(4) = P_{\mathrm{DIES}}(8) = 0.0625$$

$$P_{\mathrm{DIES}}(5) = P_{\mathrm{DIES}}(7) = 0.25$$

$$P_{\mathrm{DIES}}(6) = 0.375$$

is different from (although very close to) the maximum entropy $S_{ME} \approx 1.407\,757$.

References

Aboav D A 1970 *Metallography* **3** 383–90
—— 1980 *Metallography* **13** 43–58
Billia B, Jamgotchian H and Nguyen Thi H 1991 *Metall. Trans.* A **22** 3041–50
Delannay R and Le Caër G 1992 in preparation
Fraser D P, Zuckermann M J and Mouritsen O G 1990 *Phys. Rev.* A **42** 3186–95
Fradkov V E, Shvindlerman L S and Udler D G 1987 *Phil. Mag. Lett.* **55** 289–94
Groeneveld J, Boel R J and Kasteleyn P W 1978 *Physica* **93A** 138–54
Glotzer S C, Stauffer D and Sastry S 1990 *Physica* **164A** 1–11
Grünbaum B and Shephard G C 1987 *Tilings and Patterns* (New York: Freeman)
Herrmann H J 1986 *J. Stat. Phys.* **45** 145–51
Jamgotchian H, Billia B and Nguyen Thi H 1991 *Ann. Chim. Fr.* **16** 229–35
Khatun M, Barry J H and Tanaka T 1990 *Phys. Rev.* B **42** 4398–405
Le Caër G 1991a *J. Phys. A: Math. Gen.* **24** 1307–17, 2677
—— 1991b *J. Phys. A: Math. Gen.* **24** 4655–75
Le Caër G and Delannay R 1992 *J. Phys. A: Math. Gen.* submitted
Lewis F T 1931 *The Anatomical Record* **50** 235–65
Marsaglia G, Zaman A and Tsang W W 1990 *Stat. Prob. Lett.* **8** 35–9
Mombach J C M, Vasconcellos M A Z and de Almeida R M C 1990 *J. Phys. D: Appl. Phys.* **23** 600–6
Peshkin M A, Strandburg K J and Rivier N 1991 *Phys. Rev. Lett.* **67** 1803–6
Rivier N 1985 *Phil. Mag.* B **52** 795–819
—— 1986 *Physica* **23D** 129–37
Stauffer D, Hehl F W, Winkelmann W and Zabolitzky J G 1988 *Computer Simulation and Computer Algebra* (Berlin: Springer)
Stauffer D 1991 *J. Phys. A: Math. Gen.* **24** 909–27
Telley H 1989 *PhD Thesis* EPFL, Lausanne, Switzerland
Thompson D'A W 1917 *On Growth and Form* (Cambridge: Cambridge University Press)
Vichniac G Y 1984 *Physica* **10D** 96–116
Weaire D 1974 *Metallography* **7** 157–60
Weaire D and Rivier N 1984 *Contemp. Phys.* **25** 59–99